JOURNAL OF MATERIALS SCIENCE 31 (1996) 6089–6094

The formation of zircon from amorphous $ZrO_2 \cdot SiO_2$ powders

P. TARTAJ, C. J. SERNA, J. S. MOYA, J. REQUENA, M. OCAÑA
Instituto de Ciencia de Materiales de Madrid (C.S.I.C.), 28049 Cantoblanco Madrid, Spain
S. DE AZA
Instituto de Cerámica y Vidrio (C.S.I.C.), Arganda del Rey, Madrid, Spain
F. GUITIAN
Instituto de Cerámica, Universidad de Santiago, Santiago de Compostela, Spain

The different factors affecting the mechanism of zircon formation from amorphous $ZrO_2 \cdot SiO_2$ powders have been studied. It was shown that zircon was formed by solid state reaction between tetragonal zirconia and silica (amorphous and cristobalite). The previously suggested Hedvall effect associated with the crystallization of amorphous silica into cristobalite did not play any role in this reaction. A high degree of Si–Zr mixing in the starting amorphous powders did not affect the mechanism of zircon formation, but speeded up the reaction rate due to the small particle size of the zirconia and silica particles segregated previously to zircon formation. It was also found that the formation reaction was retarded by the presence of carbonaceous species coming from the alkoxide precursors, which were probably retained at grain boundaries after calcination, acting as a diffusion barrier. These factors can explain the observed differences in the temperatures of zircon formation previously reported.

1. Introduction

Because of its high chemical and phase stability (no crystallographic transformation occurs until its dissociation at ~1670 °C), low thermal expansion coefficient and high resistance to thermal shock, zircon ($ZrSiO_4$) is an important refractory material, which also finds applications as a ceramic matrix for high-temperature pigments [1]. Recently, several procedures have been reported for the preparation of high-purity zircon powders, including the sol–gel process [2–5] and other methods based on chemical reactions in aerosols [6–8]. All these methods produce amorphous $ZrO_2 \cdot SiO_2$ powders which are further heat treated to develop crystalline zircon.

A wide range of temperatures for zircon formation from amorphous powders have been reported, depending on the preparation conditions [2–10]. Thus, the lowest temperature found for complete zircon formation is about 1250 °C (with a holding time of 2 h) [2], whereas in some cases, zircon was not completely developed even after heating at 1650 °C for 2 h [3]. To explain these differences, an evaluation of the factors that influence the formation process is required. Although they have not been well established, several suggestions have been made in the literature. Thus, the formation of zircon has been proposed to be accelerated by the presence of the Hedvall effect, associated with the crystallization of amorphous silica into cristobalite [3, 10]. It has also been indicated the convenience of having a high degree of Si–Zr mixing in the starting powders to favour the crystallization process [11], as it occurs in the formation of mullite from silica–alumina powders. It is well known that in this system, a good Si–Al mixing results in the crystallization of mullite at a low temperature (900 °C), directly (without silica and alumina segregation) from the $SiO_2 \cdot Al_2O_3$ amorphous precursor after a reorganization of bonds [12]. Kanno [3] has also argued about the nature of the zirconia phase (tetragonal or monoclinic) involved in the reaction of zircon formation, suggesting that although the tetragonal phase (t-ZrO_2) is more favourable for zircon formation, the only reacting phase at high temperature (>1550 °C) is the monoclinic one (m-ZrO_2). Finally, the positive influence of seeding on lowering the crystallization temperature of zircon has also been reported [2, 5, 10].

The aim of this work was to study the factors affecting the formation of zircon from amorphous precursors in the absence of seeding, paying particular attention to the nature of the reacting zirconia phase and degree of Si–O–Zr mixing in the starting powder. For this purpose, a detailed study of the zircon crystallization process from an amorphous $ZrO_2 \cdot SiO_2$ powdered sample, prepared by hydrolysis of an aerosol, was carried out. The important effect of the organic species, present in the starting amorphous powder, on zircon formation was particularly emphasized.

0022–2461

2. Experimental procedure

The amorphous $ZrO_2 \cdot SiO_2$ powder was prepared by hydrolysis of a liquid aerosol, consisting of a mixture of silicon tetraethoxide (TEOS) and zirconium *n*-propoxide, following a procedure previously described [7]. To study the effect of the Si–Zr mixing in the starting powder on zircon formation, spherical particles of amorphous silica (mean diameter 0.6 μm), prepared by hydrolysis of an ethanolic TEOS solution in the presence of ammonia [13], and amorphous zirconia powder (mean particle size 0.2 μm) obtained by hydrolysis of a zirconium *n*-propoxide solution in ethanol, were also used.

Chemical analysis of the amorphous $ZrO_2 \cdot SiO_2$ powder was carried out by plasma emission (ICP, Jobin-Ivon, JY-38 VHR). Carbon determination in the samples was carried out in a Fisons-EA1108 analyser. Scanning electron microscopy (SEM, Zeiss, DSM 960) was used to examine the morphology and size distribution of the $ZrO_2 \cdot SiO_2$ particles.

The infrared spectra (Nicolet 20SXC) of the samples were recorded using a KBr matrix. Thermogravimetric (TGA) and differential thermal (DTA) analyses (Netsch, STA 409) were performed in an air atmosphere at a heating rate of $10\,^{\circ}C\,min^{-1}$.

High-temperature X-ray diffraction was carried out in a Siemens D5000 apparatus equipped with a HTK camera (Anton Park). The sample was heated at a rate of $10\,^{\circ}C\,min^{-1}$ and kept for 1 h at the desired temperature before diffraction experiments. For normal X-ray diffraction at room temperature, a Philips PW 1710 diffractometer was used.

The fraction of zircon formed in the calcined powders (α_{ZrSiO_4}) was evaluated from the relative intensities, I, of the X-ray diffraction peaks obtained at room temperature for zircon (2 0 0) and tetragonal (1 0 1) and monoclinic (1 1 1, 1 1 $\bar{1}$) zirconias, using the expression [14]

$$\alpha_{ZrSiO_4} = \frac{I_{Z(200)}}{I_{Z(200)} + I_{T(101)} + I_{M(111)} + I_{M(11\bar{1})}} \quad (1)$$

For calcination, the solids were placed in a platinum crucible and kept for different periods of time in a furnace heated at the desired temperature.

An estimation of the crystallite size of tetragonal ZrO_2 in the calcined samples was obtained from X-ray diffraction by applying the Scherrer formula to the (1 0 1) reflection (2θ at ~30.28°).

To eliminate the organic species present in the as-prepared $ZrO_2 \cdot SiO_2$ powder, a certain amount of sample was dispersed in doubly distilled water by sonication. The resulting dispersion was then centrifuged and the supernatant discarded. This procedure was repeated several times, after which the final precipitate was dried at 50 °C.

3. Results and discussion

3.1. Characterization of the amorphous precursor

The as-prepared $ZrO_2 \cdot SiO_2$ amorphous powder consisted of spherical particles having a mean diameter of 0.6 μm (Fig. 1). Its chemical composition is presented in Table I. The infrared spectrum (Fig. 2) of this powder showed two strong bands at ~1000 and 455 cm^{-1} mainly due to Si–O and Zr–O vibrations, respectively. The Si–O absorption appears overlapped with peaks at 1046, 1008 and 968 cm^{-1}, which along with those in the 3000–2800 and 1300–1150 cm^{-1} regions, reveal the presence in the powder of organic impurities coming from residual alkoxide groups and adsorbed alcohols produced in the hydrolysis reaction [7]. These bands disappeared after washing the sample with doubly distilled water, the Si–O band then being observed at 990 cm^{-1} (Fig. 2). The low frequency of the latter when compared with the same kind of vibration in amorphous silica (~1100 cm^{-1}) [15] indicates the existence of a high degree of Si–O–Zr mixing in the sample [7]. Finally, the strong absorptions at 3380

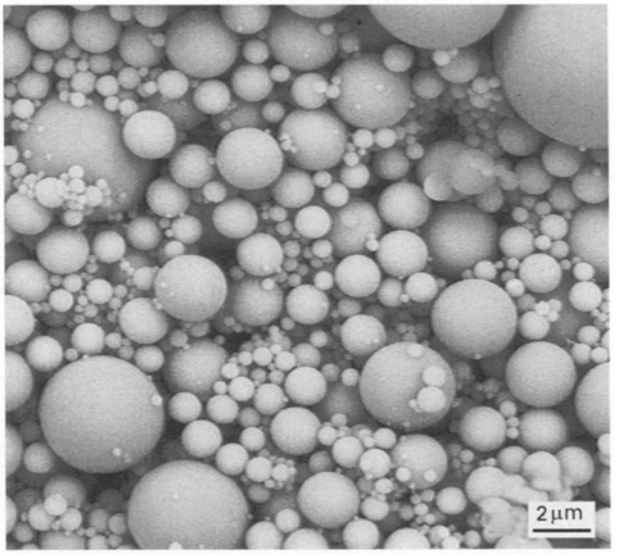

Figure 1 Scanning electron micrograph of the $ZrO_2 \cdot SiO_2$ sample.

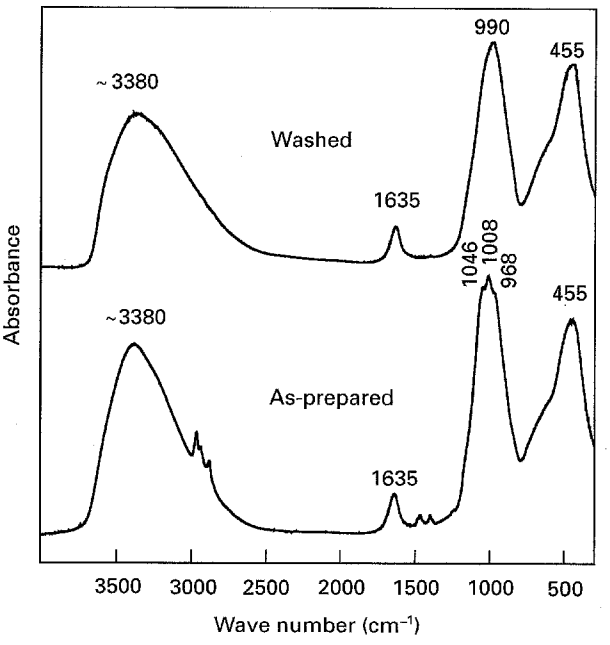

Figure 2 Infrared spectra of the $ZrO_2 \cdot SiO_2$ sample as-prepared and after washing.

and 1635 cm^{-1} are indicative of a high water content in the particles.

The DTA curve of the sample (Fig. 3) showed two strong endothermic peaks at 120 and 310 °C due to the release of adsorbed water and alcohols, followed by an exothermic effect at 320 °C, which is attributed to the decomposition of residual organic species (residual alkoxide groups and alcohols). The total weight loss between 25 and 500 °C associated with these processes was 36 wt % (Fig. 3). An additional exothermic peak appeared at 905 °C, which is due to the crystallization of tetragonal zirconia (t-ZrO_2), as was further confirmed by high-temperature X-ray diffraction (Fig. 4). It should be noted that a weight loss of 1.2 wt % is still observed between 900 and 1500 °C, being more pronounced in the interval 900–950 °C and slighter at higher temperature. The origin of this process will be further addressed.

3.2. Zircon formation

Fig. 4 shows the high-temperature X-ray diffraction patterns of the $ZrO_2 \cdot SiO_2$ sample, recorded between 900 and 1500 °C. Below 900 °C, the powder was found to be amorphous, whereas the crystallization of t-ZrO_2 was detected at 900 °C. The phase transformation from metastable tetragonal to monoclinic ZrO_2, usually observed in zirconia powders in the range 600–1000 °C [16, 17], was not observed in this sample. The inhibition of this phase transformation could be

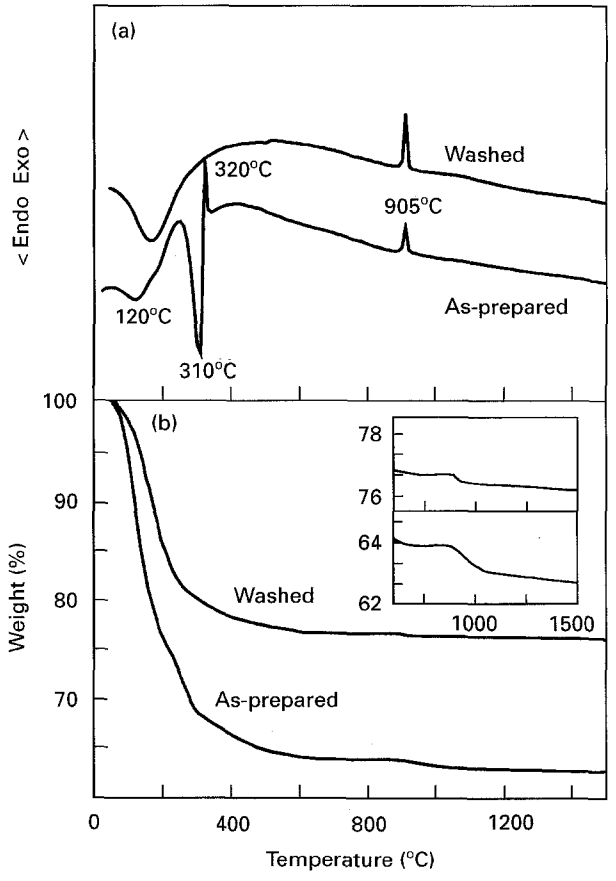

Figure 3 (a) Differential thermal and (b) thermogravimetric analyses of the $ZrO_2 \cdot SiO_2$ sample as-prepared and after washing.

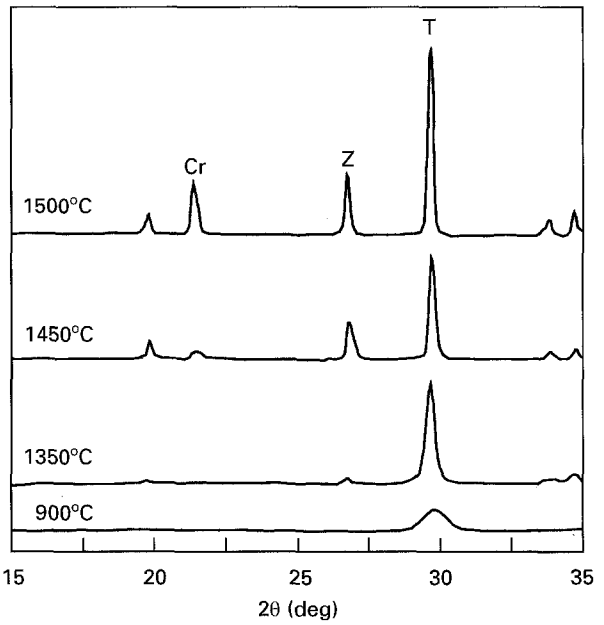

Figure 4 High-temperature X-ray diffraction patterns obtained at different temperatures for the as-prepared $ZrO_2 \cdot SiO_2$ sample. The symbols designating the main reflections of different phases are: Z, zircon; T, tetragonal zirconia; Cr, cristobalite.

ascribed to a blocking effect of silica which would hinder the growth of zirconia particles, keeping them below their critical size (30 nm) [18]. Above ~1100 °C, it is well known that the only stable phase is the tetragonal one [19]. Therefore, the zirconia phase involved in the zircon formation is always the tetragonal one, and any consideration on the nature of the zirconia phase involved in the zircon formation from amorphous powders, as that reported by Kanno [3], must be disregarded. The monoclinic zirconia observed by this author by room-temperature X-ray diffraction after heating a sol–gel prepared $ZrO_2 \cdot SiO_2$ sample at >1550 °C, must have been formed in the cooling process.

It is also clear from Fig. 4 that the crystallization of zircon starts at 1350 °C, whereas the first traces of cristobalite appeared at 1450 °C. At higher temperature (1500 °C), the amount of cristobalite increases faster than that of zircon (Fig. 4). These results clearly indicate that the previously suggested Hedvall effect associated with the crystallization of silica [3, 10] is not present in the zircon formation, which is not surprising, because this effect is always associated with a displacive polymorphic transition (i.e. α–β quartz) [20] rather than to a crystallization process involving a reconstructive transformation as occurs in the case of silica gel–β cristobalite. Further confirmation is afforded by the X-ray diffraction patterns obtained after calcining at 1550 °C two samples with different Si/Zr atomic ratios (Fig. 5), which showed that the amount of zircon formed was significantly smaller in the sample having an excess of silicon (Si/Zr = 1.85) than in the stoichiometric one.

The segregation of zirconia and silica before zircon crystallization, even in samples having a high degree of Si–Zr mixing in the precursor, indicates that in this system, the mixed oxide formation always takes place

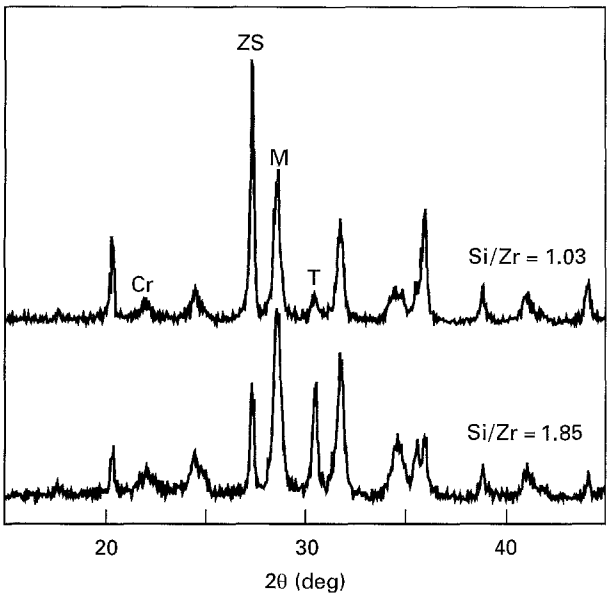

Figure 5 X-ray diffraction patterns obtained after heating at 1550 °C for 2 h, two $ZrO_2 \cdot SiO_2$ powders with different Si/Zr atomic ratio. The symbols designating the main reflections of different phases are: ZS, zircon; T, tetragonal zirconia; M, monoclinic zirconia; Cr, cristobalite.

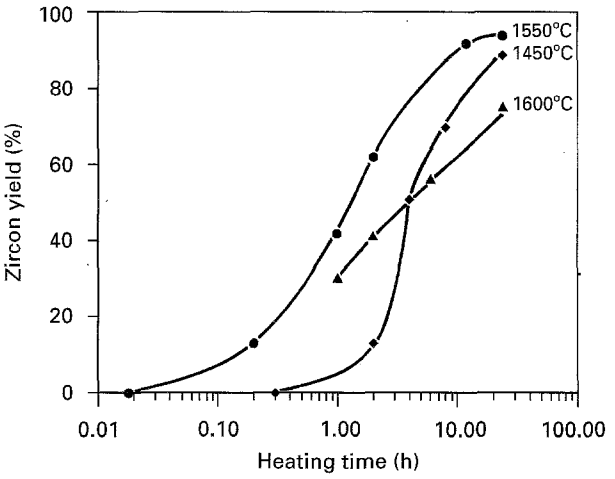

Figure 6 Zircon yield as a function of heating time for the $ZrO_2 \cdot SiO_2$ sample calcined at different temperatures.

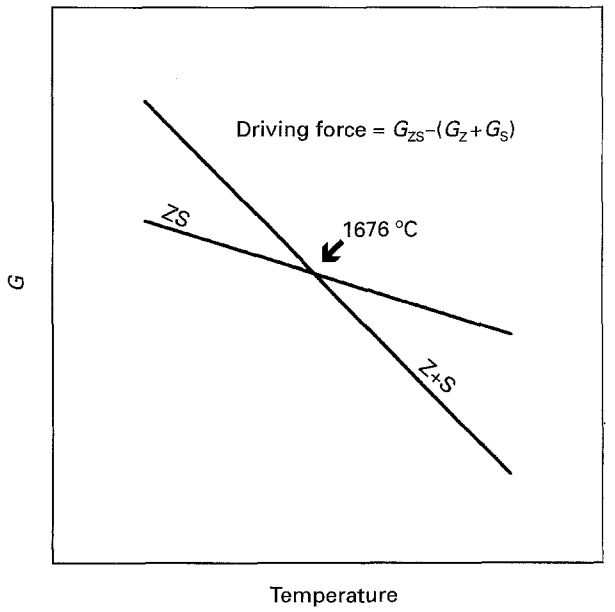

Figure 7 Qualitative variation with temperature of the free energy of zircon, G_{zircon}, and of the mixture of SiO_2, G_{SiO_2}, and ZrO_2, G_{ZrO_2} (from [21]).

by solid-state reaction between the two constituents, silica and zirconia. This is contrary to other cases such as the silica–alumina system, in which a good Al–Si mixing favours direct mullite crystallization without phase segregation [12]. Therefore, the zircon formation is governed by the factors affecting a solid-state reaction controlled by diffusion, i.e. temperature, holding time, particle size and the presence of impurities.

In our sample, the effects of heating time and temperature on zircon crystallization are shown in Fig. 6, in which the zircon yield is plotted against heating time at different temperatures. The obtained "S"-shaped curves, characteristic of a nucleation and growth mechanism, in which the controlling step is nucleation, are similar to those reported by Mori *et al.* [5] using a $ZrO_2 \cdot SiO_2$ colloidal gel. Fig. 6 indicates that the rate of zircon formation increases with temperature up to 1550 °C, decreasing at still higher temperature (1600 °C). This behaviour could be explained by comparing the qualitative variation with temperature of the free energy of zircon with that of the mixture of SiO_2 and ZrO_2 (Fig. 7). It is well known that the driving force for reaction to occur is given by the difference in free energy between the reaction products and the reactants. Obviously, in our case, the difference $G_{zircon} - (G_{SiO_2} + G_{ZrO_2})$ decreases when approaching the zircon dissociation temperature (~1670 °C). Therefore, although thermodynamically the zircon formation reaction is still favourable at 1600 °C, the kinetic would slow down as a consequence of the decrease in the magnitude of the driving force. This explanation would also justify previous observations, according to which no appreciable progresses in zircon formation took place when heating $ZrO_2 \cdot SiO_2$ samples above 1550 °C [3]. It should be noted that the small amount of alumina contained in our sample, 0.67% by weight (Table I), can form a silica-rich liquid phase at about 1550 °C [21], which could also have a decreasing effect on the yield of zircon formation above this temperature.

Impurities are known to affect diffusion in solid-state reactions. In addition to alumina, the only appreciable inorganic impurity present in our sample is hafnia (2.67 % by weight, Table I), which it is well known to behave similarly to zirconia and therefore, it does not play an important role in zircon formation. As has been stated, the starting $ZrO_2 \cdot SiO_2$ powder also contains a high amount of organic species (3.1 % by weight of carbon, Table I). To analyse the influence of such kinds of impurities in the formation of zircon, the reaction rate in the as-prepared sample was compared with that in a sample washed before calcination to eliminate these impurities. This elimination was confirmed by the absence in the DTA curve of the endothermic and exothermic peaks at about 300 °C,

TABLE I Composition (wt %) of the amorphous $ZrO_2 \cdot SiO_2$ sample

ZrO_2	SiO_2	Fe_2O_3	TiO_2	Al_2O_3	CaO	HfO_2	Na_2O	Carbon[a]
65.48	31.01	0.06	0.03	0.67	0.03	2.67	0.05	3.10

[a] Corresponding to organic impurities (adsorbed alcohols and residual alkoxides groups).

ascribed to the organic impurities (Fig. 3), and by the decrease in weight losses detected by TGA with respect to the unwashed sample (Fig. 3). The comparison between the zircon formation rate at a given temperature (1450 °C) in both samples (Fig. 8) clearly manifested that the formation reaction was slower in the as-prepared sample. It should be noted that a slight weight loss was observed by TGA between 900 and 1500 °C (Fig. 3), which was higher for the as-prepared sample (1.2 wt %) than for the washed one (0.5 wt %). This weight loss could be related to residual carbonaceous species still retained in the sample, much probably at the zirconia–silica grain boundaries, acting as a diffusion barrier, thus explaining the higher temperature of zircon formation in the unwashed sample. The carbon analysis carried out in both the as-prepared and washed samples, just before zircon formation (1250 °C), strongly supports the previous statement. Thus, a carbon content of 500 p.p.m. was measured for the as-prepared sample, whereas the amount of carbon was negligible (<10 p.p.m.) in the washed one. In this new context, some observations reported in the literature, such as, for example, the higher zircon crystallization rate detected by Vilmin *et al.* [2] for a diphasic $ZrO_2 \cdot SiO_2$ gel when compared with a monophasic one, could be explained. Thus, in agreement with the above interpretation, the diphasic gel was prepared from inorganic compounds in the absence of organic reagents, whereas the monophasic one was prepared using silicon ethoxide, and therefore it should have contained some carbonaceous impurities.

It is noteworthy that the organic impurities present in amorphous precursors prepared from alkoxides have also been shown to play an important role in the crystallization behaviour of several other simple and mixed oxides (TiO_2 [22], HfO_2 [23], mullite [24]). Therefore, the presence of such kinds of impurities should be taken into account when studying ceramic systems prepared from metal alkoxides.

Finally, to analyse the effect of the degree of Si–Zr mixing in the starting powder on zircon formation, the zircon yield obtained as a function of holding time for the aerosol-washed sample and for a mechanical mixture of amorphous silica (particle size = 0.6 μm) and amorphous zirconia (particle size = 0.2 μm) were compared (Fig. 8). As observed, the crystallization of zircon is much faster when starting from the aerosol-prepared amorphous powder having a high degree of Si–Zr mixing. This is explained by the crystallite size of t-ZrO_2 present in this powder at the beginning of zircon formation (1300 °C), which, as determined from the Scherrer equation (70 nm), is much smaller than the particle size of the zirconia used in the mechanical silica–zirconia mixture (0.2 μm), thus increasing the contact area between reacting particles, and therefore favouring diffusion. Therefore, the Si–Zr mixing in starting $ZrO_2 \cdot SiO_2$ affects the zircon formation process in the sense that it gives rise to small zirconia particles after segregation, which favours diffusion.

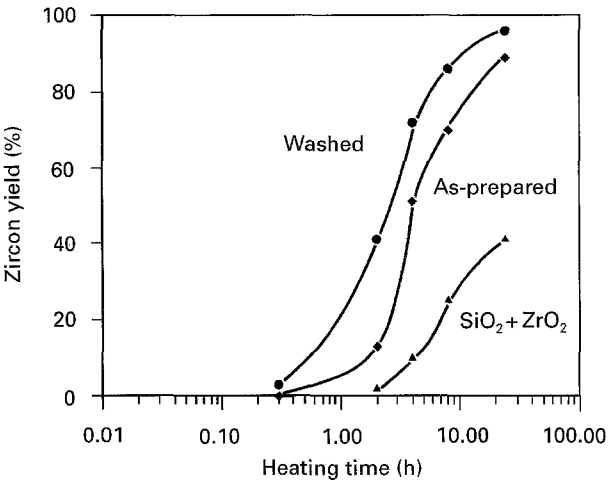

Figure 8 Zircon yield at 1450 °C as a function of heating time calculated for the $ZrO_2 \cdot SiO_2$ sample, as-prepared and after washing; and for a mechanical silica–zirconia mixture.

4. Conclusion

The formation of zircon from amorphous $ZrO_2 \cdot SiO_2$ powders takes place by solid-state reaction between tetragonal zirconia and silica (amorphous and cristobalite), with no contribution of the previously suggested Hedvall effect associated with the crystallization of amorphous silica into cristobalite. This mechanism is independent of the degree of Si–Zr mixing of the starting precursor, because silica and zirconia segregate before zircon formation. A high degree of mixing gives rise to segregation of small zirconia particles, which favours diffusion, thus increasing the zircon formation rate. It has also been shown that the carbonaceous species coming from the alkoxide precursors, still remain in the sample after calcination, which thus retards the zircon formation process. These factors can also explain the observed differences in the temperatures of zircon formation previously reported.

Acknowledgement

This work has been supported by the Spanish Comisión Interministerial de Ciencia y Tecnología under Projects MAT92-0328 and MAT94-0974.

References

1. F. T. BOOTH and G. N. PEEL, *Trans. J. Br. Ceram. Soc.* **61** (1962) 359.

2. G. VILMIN, S. KOMARNENI and R. ROY, *J. Mater. Sci.* **22** (1987) 3556.
3. Y. KANNO, *ibid.* **24** (1989) 2415.
4. T. MORI and H. YAMAMURA, *J. Am. Ceram. Soc.* **75** (1992) 2420.
5. T. MORI, H. YAMAMURA, H. KOBAYASHI and T. MITAMURA, *J. Mater. Sci.* **28** (1993) 4970.
6. S. S. JADA, *J. Mater. Sci. Lett.* **9** (1990) 565.
7. P. TARTAJ, J. SANZ, C. J. SERNA and M. OCAÑA, *J. Mater. Sci.* **29** (1994) 6533.
8. P. TARTAJ, T. GONZÁLEZ-CARREÑO, J. SANZ, C. J. SERNA and M. OCAÑA, *Adv. Sci. Tech.* **3B** (1995) 1211.
9. T. ITOH, *J. Crystal Growth* **125** (1992) 223.
10. Y. SHI, X. X. HUANG and D. S. YAN, *J. Eur. Ceram. Soc.* **13** (1994) 113.
11. Y. KANNO and T. SUZUKI, *J. Mater. Sci. Lett.* **8** (1989) 41.
12. I. A. AKSAY, D. M. DABBS and M. SARIKAYA, *J. Am. Ceram. Soc.* **74** (1991) 2343.
13. G. H. BOGUSH, M. A. TRACY and C. F. ZUKOSKI, *J. Non-Cryst. Solids* **104** (1988) 95.
14. R. C. GARVIE and P. S. NICHOLSON, *ibid.* **55** (1972) 303.
15. M. OCAÑA, V. FORNÉS and C. J. SERNA, *J. Non-Cryst. Solids* **107** (1989) 187.
16. M. I. OSENDI, J. S. MOYA, C. J. SERNA and J. SORIA, *J. Am. Ceram. Soc.* **68** (1985) 135.
17. M. OCAÑA, V. FORNÉS and C. J. SERNA, *Ceram. Int.* **18** (1992) 99.
18. V. S. NAGARAJAN and K. J. RAO, *J. Mater. Sci.* **24** (1989) 2140.
19. R. RUH and T. J. ROCKETT, *J. Am. Ceram. Soc.* **53** (1970) 360.
20. W. KINGERY, H. K. BOWEN and D. R. UHLMANN, "Introduction to Ceramics" (Wiley, New York, 1976) p. 425.
21. P. PENA and S. DE AZA, *J. Mater. Sci.* **19** (1984) 135.
22. M. OCAÑA, J. V. GARCÍA-RAMOS and C. J. SERNA, *J. Am. Ceram. Soc.* **75** (1992) 2010.
23. M. OCAÑA, M. ANDRES and C. J. SERNA, *Coll. Surface. A* **79** (1993) 169.
24. M. OCAÑA, J. SANZ, T. GONZÁLEZ-CARREÑO and C. J. SERNA, *J. Am. Ceram. Soc.* **76** (1993) 2081.

Received 4 April 1995
and accepted 13 June 1996